Longitudinal mode selection in laser cavity by moiré volume Bragg grating

Daniel Ott*[a], Vasile Rotar[a], Julien Lumeau [a], Sergiy Mokhov [a], Ivan Divliansky [a], Aleksandr Ryasnyanskiy[b], Nikolai Vorobiev[a], Vadim Smirnov[b], Christine Spiegelberg[b], Leonid Glebov[a]
[a]CREOL, College of Optics and Photonics, 4000 Central Florida Blvd., Orlando, FL USA 32816;
[b]Optigrate Corporation, 3267 Progress Drive, Orlando, FL USA 32826

ABSTRACT

A Fabry-Perot etalon, consisting of two π phase shifted reflecting volume Bragg gratings, is presented. These gratings are obtained as a moiré pattern resulting from sequential recording of interference patterns with different periods in photo-thermo-refractive glass and called moiré volume Bragg gratings (MVBGs). A detailed investigation of the fundamental operating principles and measurement techniques for phase shifted gratings is shown. Experimental results demonstrating a MVBG with a 15 pm bandwidth and 90% transmission at resonance are presented. The use of the MVBG for longitudinal mode selection in a laser resonator is shown.

Keywords: Spectral filter, single frequency, mode selector, holography

1. INTRODUCTION

Narrow bandwidth sources find many applications in the fields of spectroscopy, metrology, WDM communication systems and optical sensor networks. Thin film filters and Fabry-Perot etalons are commonly used to create narrow bandwidth filters with large apertures[1,2]. Bragg gratings and phase-shifted gratings (PSGs) are employed for fiber based filters, most prominently appearing in Distributed Bragg Reflector and Distributed Feedback lasers[3,4]. However, until recently, no experimental demonstrations of PSGs were performed outside of fibers due to the unavailability of bulk photosensitive materials with high optical homogeneity. Recent development in the use of photo-thermo-refractive (PTR) glass for recording volume holographic elements has led to the production of high efficiency volume Bragg gratings[5]. The main advantage of such elements is that they allow for narrowband filters in both spectral and angular spaces and are suitable for high power laser applications. This allows high efficiency reflecting Bragg gratings (RBG) to be recorded in several millimeter thick pieces of glass with losses below 1%.

Recording a PSG into a bulk medium can be achieved most efficiently by using a sequential recording of two volume Bragg gratings with grating vectors of different magnitude, but otherwise collinear. The two gratings of different spatial frequency produce a moiré pattern which consists of a high spatial frequency refractive index modulation and a slowly varying envelope[6]. The location of zero envelope amplitude induces a π phase shift in the rapidly varying refractive index modulation. When this phase shift is located in the center of a grating with a total thickness of two moiré semi-periods, a Fabry-Perot etalon resonance condition is produced. The result is a narrow bandwidth transmission peak in the center of the RBG spectrum.

A 50 pm bandwidth, moiré volume Bragg grating (MVBG), was recently demonstrated by using volume hologram recording in bulk PTR glass[7]. A filter with a bandwidth of 15 pm is presented here for use in a laser cavity to select longitudinal modes. Relevant theory for calculating the spectral response of apodized and phase shifted gratings is presented along with experimental data regarding filter performance.

2. THEORY

2.1 Coupled wave theory for non-uniform gratings

The most common method for modeling the spectral and angular response of a volume Bragg grating element is coupled wave theory (CWT) developed by Kogelnik[8]. This method predicts results closely matched to experiment with low

Laser Resonators, Microresonators, and Beam Control XIV, edited by
Alexis V. Kudryashov, Alan H. Paxton, Vladimir S. Ilchenko, Lutz Aschke, Kunihiko Washio,
Proc. of SPIE Vol. 8236, 823621 · © 2012 SPIE · CCC code: 0277-786X/12/$18 · doi: 10.1117/12.909465

computational effort. In the present work, only unslanted reflecting Bragg grating (RBG) geometry is of concern. The index modulation profile of a typical MVBG is shown in figure 1.

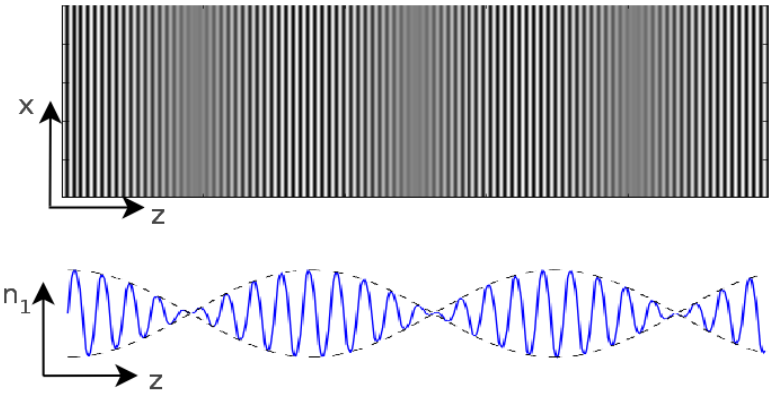

Figure 1. A schematic showing a MVBG. The axial profile of the grating shows the sinusoidal envelope with an exaggerated high frequency grating period to show detail.

In order to accurately describe the spectral response of the grating with non-uniform refractive index modulation, the slowly varying envelope approximation (SVEA) must be employed. In this approximation, the low frequency envelope must have a frequency many times less than the resonant frequency of the grating. For gratings discussed here the ratio is on the order of 10^4 making SVEA valid. Therefore, the grating can be described using a successive application of the results of CWT. The grating is divided into equal sections and the average refractive index modulation (n_1) is used in determining the response for each section of grating. To facilitate fast calculations, the results of CWT can be reformulated into transfer equations or matrices[9,10]. The following matrix formulation by Mokhov et al, is used to describe the spectral response of a given section of grating[11].

$$M(z)=\begin{bmatrix}[\cosh\gamma L+i\Delta\beta L\sinh\gamma L/(\gamma L)]\exp(i\beta_0 L) & i\kappa L\sinh\gamma L\exp(i(\beta_0 L+\phi))/(\gamma L)\\ -i\kappa L\sinh\gamma L\exp(-i(\beta_0 L+\phi))/(\gamma L) & [\cosh\gamma L-i\Delta\beta L\sinh\gamma L/(\gamma L)]\exp(-i\beta_0 L)\end{bmatrix} \quad (1)$$

Where $\Delta\beta=\beta-\beta_0$, $\gamma=\sqrt{\kappa^2-\Delta\beta^2}$, $\kappa=\pi n_1/\lambda$. The term β represents the wavenumber of incident light, with the subscript 0 representing the Bragg condition, L is the length of the grating section, and φ is a phase term used to represent the phase shift of any given section of grating. At each section of the grating the average refractive index modulation is determined and if the section contains a zero in the envelope pattern a phase of φ=π is used.

The final reflection spectrum can be calculated by successive multiplication of each grating section and the final spectrum is given by calculating

$$R(\lambda)=\left|\frac{M_{21}}{M_{22}}\right|^2 . \quad (2)$$

2.2 Design

The critical parameters of a typical moiré grating, as predicted by matrix CWT, are shown in figure 2. The simulated MVBG uses parameters of λ_0 =1064 nm, Δλ= 135 pm, n1= 180 ppm, n2=130 ppm. This gives a grating with total length of 5.5 mm. The full width at half maximum (FWHM) of the resulting resonance is 8 pm.

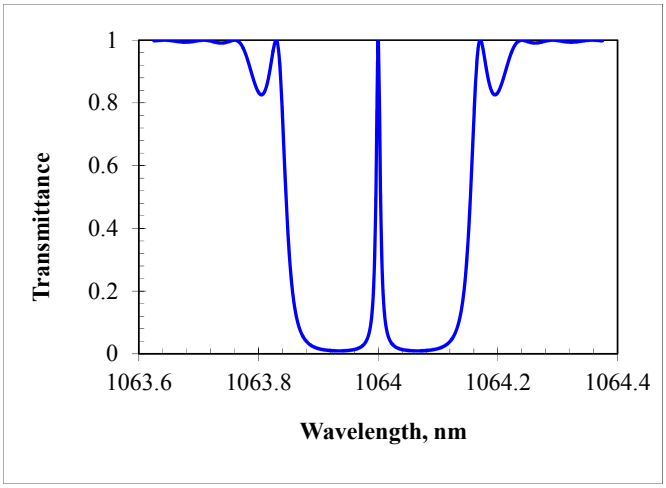

Figure 2. Theoretical transmission spectrum of a MVBG with transmission bandwidth of 10 pm. Parameters are n1=n2=180 ppm and grating thickness of 5.5 mm

The design curve for the spectral width of an MVBG is shown in figure 3. It is possible to achieve spectral widths well below 10 pm using parameters typical for volume Bragg gratings in PTR glass.

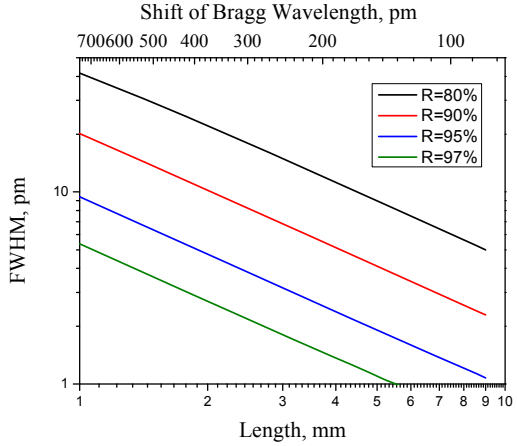

Figure 3. Dependence of spectral width of MBG on thickness. The thickness of the grating is determined by the envelope semi-period. Various curves represent the reflectance of each semi-period and can be used to calculate the desired index modulation for a given reflectance and length.

3. FABRICATION

3.1 Recording

The recording setup for an MVBG is essentially the same as for a uniform VBG. A single grating is recorded into the media, then the resonant wavelength is changed by modifying the angle of interference between the recording beams and a second grating is recorded into the same depth. The recording geometry used for recording in PTR glass is shown in figure 4. The source for our recording setup is a single frequency He-Cd laser, hence the resonant wavelength of recording is changed by adjusting the angles of interference while keeping the bisector constant. To record a resonant wavelength shift of 100 pm at 1064 nm, a shift in angle of 9.4 arc seconds is required.

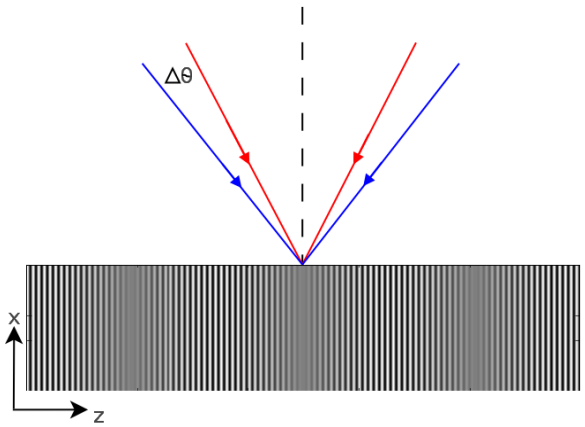

Figure 4. Two exposure recording of a moiré volume Bragg grating. The change in incidence angle between the first and second recording is 9.4 arc seconds.

3.2 Processing

The recorded grating contains the envelope in an undefined state. It is necessary to process the grating after recording to accurately determine the location of the zeros in the envelope pattern. This is accomplished by scanning the transverse axis (z axis) of the grating with a probe beam such that the grating acts as a transmission Bragg grating. The dips in the diffraction efficiency at these locations can be correlated to the points of zero envelope magnitude. From identifying these locations, the grating can be cut and polished such that the final grating contains a single envelope zero located in the center of the grating.

3.3 Measurement of grating

The transmission spectrum of the grating is measured using a tunable laser diode with sub-picometer resolution. The experimental setup is shown below in figure 5. A fiber coupled tunable laser is sent through a 3 dB coupler. One arm probes the grating with a collimated beam, while a power detector measures the transmission through the grating. The unused arm of the coupler is used to monitor back reflection from the sample to ensure that the grating is characterized at normal incidence.

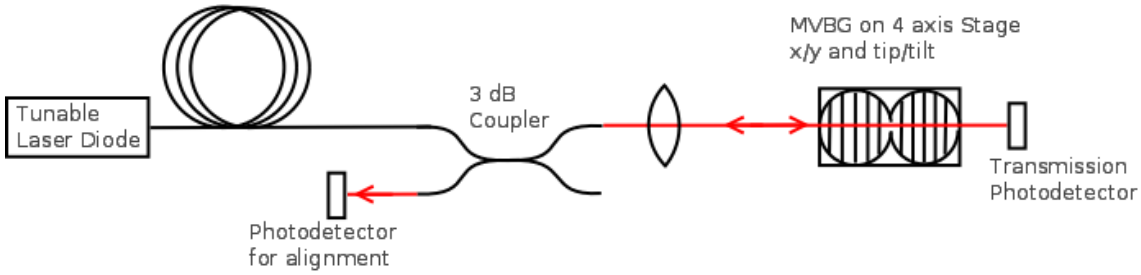

Figure 5.The setup for characterization of the spectral transmission of an MVBG with a high resolution tunable laser. A 3 dB coupler is used to determine alignment by monitoring the intensity of back reflection from the gratings rejection band.

The resultant transmission spectrum of the MVBG is shown in figure 6. It shows experimental data as well as a theoretical fit using matrix CWT. The width of the transmission peak is 15 pm FWHM and rejection band is 254 pm FWHM. The filter has a rejection ratio of -13 dB. The spectrum shows a distinct asymmetry about the resonant peak. It was found that this asymmetry is primarily due to a mismatch in the recording dosages. By inducing a mismatch in the strength of the refractive index modulation (RIM) we are able to predict the level of error in our exposure and model the results. The mismatch in RIM is 50 ppm from the specified value. Excellent coincidence between experimental results and the theory can be seen in the region of the pass band and rejection band of our filter.

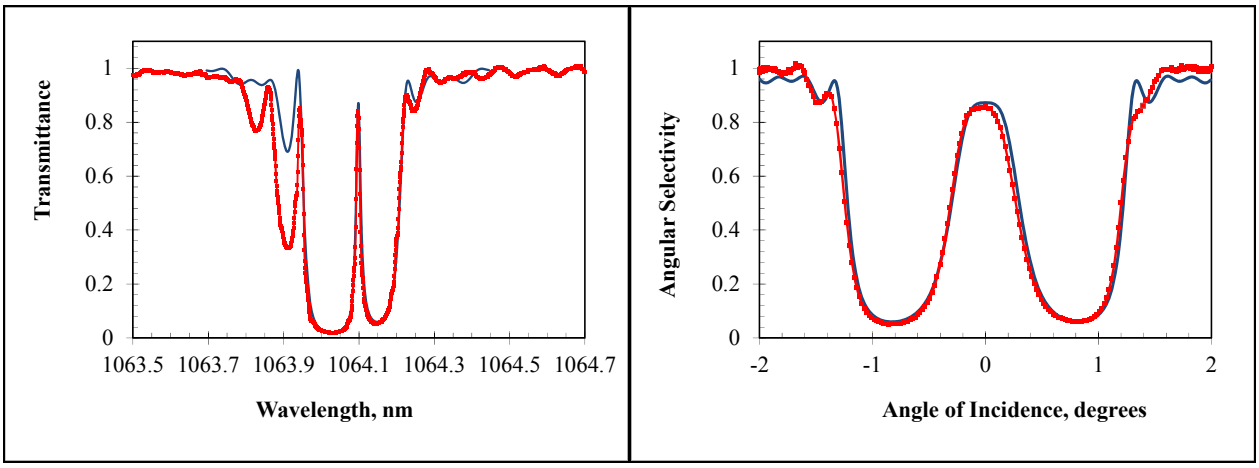

Figure 6. Transmission spectra (A) and angular selectivity (B) of a moiré Bragg grating in PTR glass. Length = 5.3 mm, refractive index modulation n1=126 ppm, n2=234 ppm. Blue – theory, red – experiment.

4. MVBG FOR MODE SELECTION

The narrow band transmission generated can be used for the generation of single frequency laser using an intracavity MVBG (figure 7). The laser cavity consists of a Yb doped fiber as the gain medium. The output is coupled into the free space cavity where the MVBG is place to achieve longitudinal mode selection. A uniform RBG with 30% reflectance is used as an output coupler. The spectral width of the output coupler is selected to match the spectral width of the MVBG such that only the modes within the resonance peak of the MVBG are allowed to resonate in the cavity. The longitudinal mode structure of the laser is characterized using a scanning Fabry Perot interferometer (SFPI). The cavity length of the laser is approximately 1.5 m resulting in a longitudinal mode spacing of 120 MHz (0.5 pm).

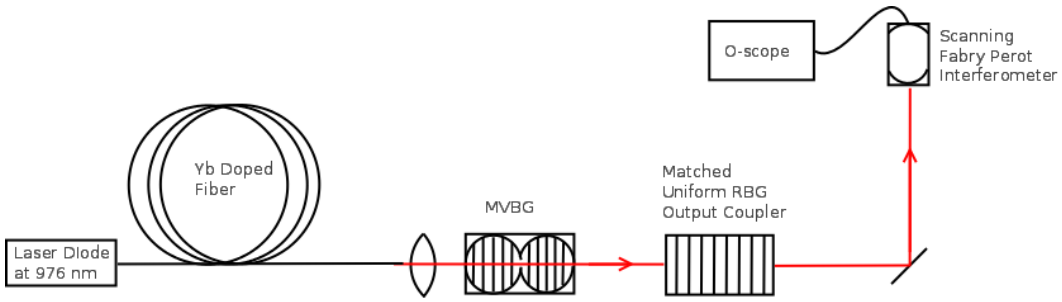

Figure 7. A fiber laser with free space section of cavity incorporating a MVBG for mode selection. A scanning Fabry Perot interferometer is used to determine the longitudinal modes present in the laser

Alignment of the MVBG is achieved by first aligning the reflection in the rejection band such that the laser is locked to the rejection band. The MVBG is then tilted so that lasing is not achieved from reflections from the MVBG. Note that the angular selectivity of the grating in figure 6 is 0.64° FWHM and over 0.3° there is a drop of only 5% in the transmission. In comparison, a tilt of tens of arc seconds is sufficient to destroy lasing off of the reflection from the rejection bands. This tilt causes no appreciable change in the filter characteristics and it is therefore acceptable to align the grating off normal incidence.

5. RESULTS

The spectral output of the laser with an intracavity MVBG was measured using an SFPI with a resolution of 7.5 MHz and a free spectral range of 1.5 GHz. Figure 8 shows the spectrum with and without the MVBG placed in the cavity. Without the filter in place, the modes fill the FSR of the etalon. The 15 pm bandwidth of the filter effectively acts as a filter with bandwidth around 2 pm due to only a very narrow region in the transmission peak of figure 6 being above lasing threshold. The filter thus allows selection of three modes from the spectrum.

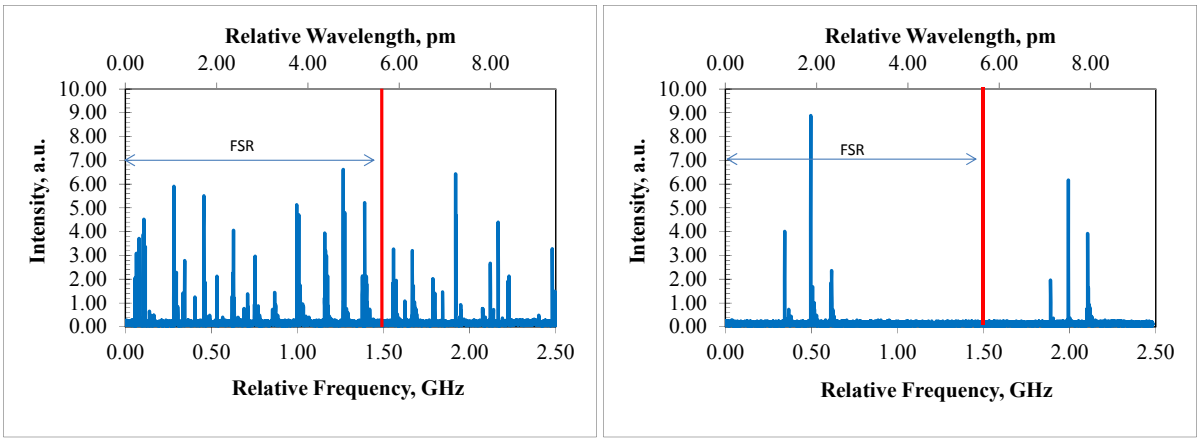

Figure 8. The spectrum of the laser from figure 7 as measured by scanning Fabry Perot etalon. Figure to the left is without MVBG and the figure on the right is with MVBG in the cavity.

6. CONCLUSIONS

A moiré volume Bragg grating with spectral FWHM of 15 pm is demonstrated with good correspondence to theory. The application of the MVBG into a laser cavity shows the potential for generating high power single frequency output. Given the current laser configuration, the number or resonating longitudinal modes is reduced to three. The primary benefit of this mode selection device is the simple alignment procedure for free space laser cavity systems. Further work will focus on fabrication of MVBG grating devices with higher transmission throughput.

REFERENCES

[1] Hendrix, K., Hulse, C., Ockenfuss, J., and Sargent, R., "Demonstration of narrowband notch and multi-notch filters," Proceedings of SPIE, vol. 7067, 706702 (2008).
[2] Mallinson, S. "Wavelength-selective filters for single-mode fiber WDM systems using Fabry-Perot interferometers," Appl. Opt., 26(3), 430-436 (1987).
[3] Kashyap, R., [Fiber Bragg Gratings], Academic Press, San Diego, 227-239 (1999).
[4] Das, B., Ricken, R., Quiring, V., Suche, H., and Sohler, W., "Distributed feedback distributed Bragg reflector coupled cavity laser with a Ti:(Fe:)Er:LiNbO3 waveguide," Opt. Lett., 29(2), 165-167 (2004).
[5] Efimov, O., Glebov, L., Smirnov, V., "High efficiency volume diffractive elements in photo-thermo-refractive glass", United States Patent 6,673,497. January 6, 2004.
[6] Reid, D., et. al., "Phase-Shifted Moiré Grating Fibre Resonators," Electronics Letters, 26(1), 10-12 (1990).
[7] Smirnov, V., Lumeau, J., Mokhov, S., Zeldovich, B., and Glebov, L., "Ultranarrow bandwidth moiré reflecting Bragg gratings recorded in photo-thermo-refractive glass," Opt. Lett. 35, 592-594 (2010).
[8] Kogelnik, H., "Coupled Wave Theory for Thick Hologram Grating," Bell System Technical Journal, 48(9), 2909-2945 (1969).
[9] Kim, S., and Fonstad, C., "Tunable narrow-band thin-film waveguide grating filters," IEEE Journal of Quantum Electronics, 15(12), 1405-1408 (1979).
[10] Yamada, M., and Sakuda, M., "Analysis of almost-periodic distributed feedback slab waveguides via a fundamental matrix approach," Appl. Opt., 26(16), 3474-3478 (1987).
[11] Glebov, L., Lumeau, J., Mokhov, S., Smirnov, V., and Zeldovich, B., "Reflection of light by composite volume holograms: Fresnel corrections and Fabry-Perot spectral filtering.," Journal of the Optical Society of America A, 25(3), 751-64 (2008).